ELSEVIER

Thermochimica Acta 323 (1998) 53–63

thermochimica acta

Strain effects on thermal transitions and mechanical properties of thermoplastic polyurethane elastomers

Dawn M. Crawford[a,*], Robert G. Bass[b,1], Thomas W. Haas[b,2]

[a] *U.S. Army Research Laboratory, Bldg. 4600 Deer Creek Loop, APG, MD 21005-5069, USA*

[b] *Virginia Commonwealth University, Department of Chemistry, 1001 West Main Street, P.O. Box 842006, Richmond, VA 23284-2006, USA*

Received 29 December 1997; received in revised form 29 June 1998; accepted 11 July 1998

Abstract

An investigation on the effect of strain on the domain structure of thermoplastic polyurethane elastomers (TPEs) is reported. Thermal characterization utilizing differential scanning calorimetry (DSC) and dynamic mechanical analysis (DMA) is presented along with mechanical properties of model TPEs before, and after, varying degrees of strain aging. Model TPEs were subjected to tensile strains between 100 and 400% elongation and aged for varying lengths of time at ambient and elevated temperatures. DSC and DMA were utilized to investigate the changes in morphology that occurred as a result of strain elongation. The effect of strain aging on the TPEs mechanical properties such as abrasion resistance is also discussed. DSC results indicated that the polymer undergoes morphology changes due to strain, resulting in some degree of phase mixing. DMA data indicated that polyester TPEs and polyether TPEs respond differently to induced strain, suggesting that domain re-ordering in these materials may occur by different mechanisms.

Keywords: Abrasion; Differential scanning calorimetry; Dynamic mechanical analysis; Morphology; Polyurethane; Strain

1. Introduction

Thermoplastic polyurethane elastomers (TPEs) are versatile materials that behave as cross-linked elastomers at room temperature but, unlike conventional elastomers, they can be processed, shaped and formed upon heating via numerous industrial processes. TPEs exhibit excellent properties, including abrasion resistance; however, because these polymers are not chemically cross-linked, TPEs exhibit lower recoverability following elongation than cross-linked elastomers. The U.S. Army utilizes TPEs as coatings on collapsible fuel and water tanks. When these tanks are empty and stored, local strains occur at folds in the TPE coating. The coating in these regions is known to exhibit reduced properties, especially abrasion resistance. Therefore, a research project was established to investigate the changes in TPE polymer structure as a result of strain. To accomplish this goal, numerous model TPEs were characterized in the original state and following strain-aging experiments. Thermal techniques such as differential scanning calorimetry (DSC) and dynamic mechanical analysis (DMA) were utilized as well as mechanical (tensile and abrasion) tests. The TPEs that were investigated are not the actual polymer compounds used as coatings on collapsible tanks, but are model polymers that have

*Corresponding author. Fax: +1-410-306-0676; e-mail: dcrawfor@arl.mil

[1]Fax: +1-804-828-8599; E-mail: rbass@saturn.vcu.edu

[2]Fax: +1-804-828-8599; E-mail: twhaas@vcu.edu

0040-6031/98/$ – see front matter
PII: S0040-6031(98)00541-3

similar structures to actual tank coatings prior to fabrication. Although the domain structure of polyurethane elastomers has been previously studied using infra-red dichroism and small angle X-ray scattering while the materials were subjected to instantaneous strains [1–6], the research presented herein is the first time that such materials have been studied using DSC and DMA after long-term strain aging. Mardel et al. [7] have previously investigated the relationship between polymer morphology and wear performance of polyether polyurethanes as a function of annealing. However, the research presented herein is novel in its focus on the relationship between strain aging and abrasion properties of polyurethane elastomers.

2. Background

Polyurethane elastomers are block polymers whose chains are composed of alternating low glass-transition temperature (T_g) 'soft' segments and rigid urethane 'hard' segments which soften much above room temperature [8]. The soft segments are most often comprised of polyester or polyether macroglycols and the hard segments are formed from the chain extension of a diisocyanate with a low molecular weight diol [8–10]. The hard and soft segments are joined end-to-end through covalent urethane bonds and, therefore, polyurethanes are classified as multi-block copolymers [11]. The differences in polarity between the hard and soft segments render these regions incompatible and the result is that they do not mix on a molecular level, producing a microphase separated structure [12–15]. The hard segment rich domain is generally characterized as semi-crystalline and provides stiffness and reinforcement to the polymer. The soft segment domains are responsible for elastic behavior and are usually amorphous with a T_g below room temperature. Formation of polyurethane elastomers is shown schematically in Fig. 1. A schematic of the phase separated structure is shown in Fig. 2.

3. Experimental

The model polymers used in the study were supplied by Goodrich. The polymers were prepared by a 'one shot' melt polymerization process and compression molded into ASTM size sheets. Three of the model polymers consist of a polyester polyol and are designated as ES1, ES2 and ES3. 'ES' indicates that the polymers were formed using a polyester macroglycol as the soft segment. The numeric designations correlate with increasing percentage of the hard segment. The macroglycol, comprising ES1, ES2 and ES3, is poly(tetramethylene adipate) glycol. The fourth model polymer is designated as ET1 and con-

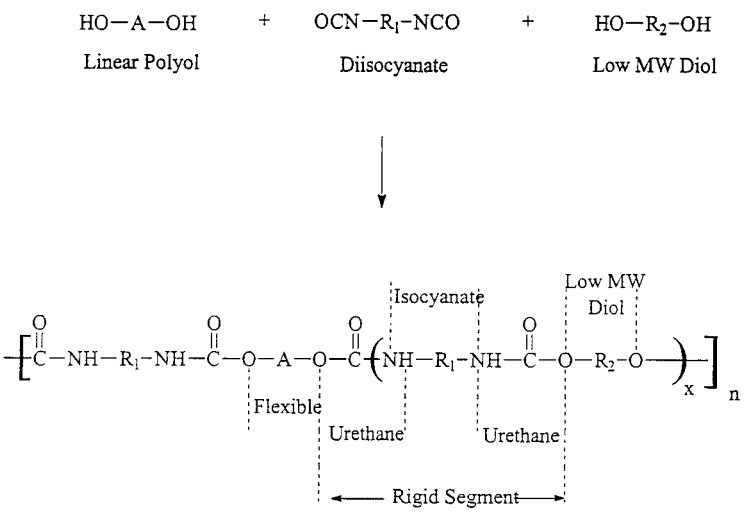

Fig. 1. Formation of polyurethane elastomer.

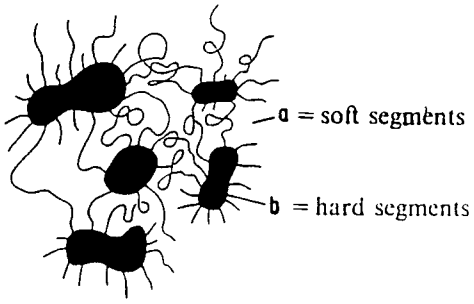

Fig. 2. Segmented structure of polyurethanes.

sists of a polyether polyol (polytetramethylene ether glycol). 'ET' indicates that the polymer was formed using a polyether macroglycol as the soft segment. ET1 has the same mole percentage of soft and hard segments as ES2. All of the model polymers are comprised of the same diisocyanate and short-chain diol (4,4′-diphenylmethane diisocyanate and 1,4-butanediol, respectively). Therefore, ES2 and ET1 differ only in the chemistry of the soft segment. The chemical structures of the starting materials are shown in Fig. 3. Table 1 shows the molar ratios of the model polymers.

Thermal analysis was performed on the model polymers before, and after, strain aging. Strain was induced by stretching the polymers at 100% intervals between 100% and 400% elongations. The samples were held at constant length throughout the aging

Table 1
Molar ratios of model polymer starting materials [a]

Model polymer	Polyol	1,4-Butanediol	MDI
ES1	1.00	0.75	1.75
ES2, ET1	1.00	1.02	2.02
ES3	1.00	1.33	2.33

[a] Molar ratios of the model polymers were provided by Goodrich.

experiment. All model polymers were strain aged at ambient (25°C ±2°C) temperature for 240 h, unless otherwise noted. After strain aging, the polymers were allowed to relax for 1 h prior to testing.

DSC measurements were conducted using a TA Instruments 2920 DSC. Experiments were conducted under a nitrogen purge of 50 cc/min. The polymers were cooled to −65°C and heated to 200°C at a heating rate of 10°/min. The sample size was ≈10 mg.

DMA experiments were performed using an Imass automated rheovibron (Toyo Instruments). Data reported in this paper were taken at 110 Hz. A high oscillation frequency was chosen to better correlate with the abrasion testing which induces a high-frequency condition. The polymers were cut to dimensions of ≈0.6 mm thick, 1.2 mm wide and 26 mm long. The samples were cooled to −100°C and heated to 100°C at a rate of 2°C/min.

Abrasion tests were conducted using a Zwick rotating drum abrasion machine according to the method

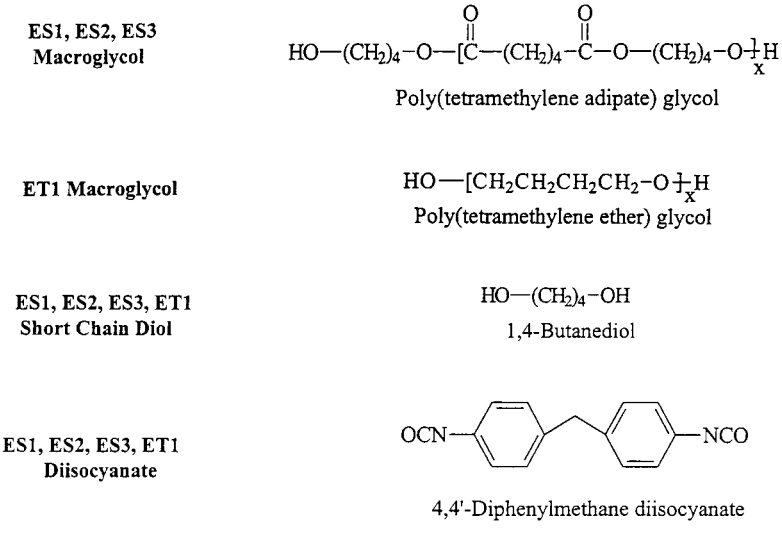

Fig. 3. Chemical structures of starting materials.

detailed in the International Standard Method (ISO) 4649. Tensile tests were performed in accordance with ASTM D412.

4. Results and discussion

DSC scans show that all of the model polymers exhibit three prominent thermal transitions including a glass transition below 0°C and two broad endothermic transitions at higher temperatures. The lower temperature endothermic transition (Endo 1) has previously been identified with disruption of soft segment/hard segment bonds [8,16] or disruption of short-range order within the hard segment microdomains [17]. The higher temperature endothermic transition (Endo 2) is related to the breakup of inter-urethane hydrogen bonds [8,16]. This series of transitions is representative of the two phases that are present in the polymer and reflect the relative amounts of hard and soft segments present. Table 2 lists the peak endothermic temperatures and ΔH associated with the transitions.

ES1, ES2 and ES3 have increasing mole percentages of hard segment. This is reflected in the DSC data of the higher temperature endothermic transition (Endo 2). As the percentage of hard segment is increased, both the peak temperature of the transition and the ΔH associated with the transition increase. ES1, ES2, and ES3 are all comprised of the same polyester polyol (MW=1000 units). The peak temperature of Endo 1 increases slightly, as does the ΔH of the transition. This change suggests that there may be increased interaction between the hard and soft segments as the hard segment content is increased. The soft segment T_g increases as the hard segment content increases. As mentioned earlier, ES2 and ET1 differ only in the chemistry of the soft segment polyol; 'ES' denoting a polyester polyol and 'ET' a polyether polyol. Both polyols have similar molecular weight ≈1000 units) and the same mole percentage of hard segment. Therefore, differences in the DSC transitions of ES2 and ET1 shown in Table 2 are specifically related to the soft segment behavior and the interaction between the hard and soft segments. This is apparent in the T_gs of ES2 and ET1. ES2 has a T_g of −32°C. ET1 has a much lower T_g that did not show up in the temperature range of the DSC experiment but is clearly seen using the rheovibron. The lower T_g of ET1 is the result of greater rotational freedom of the C–O–C bond in the polyether polyol. Another significant difference between ES2 and ET1 is seen in Endo 2 which is related to the dissociation of the inter-urethane bonds that form the hard domains. ET1 has a much higher temperature associated with this transition than ES2. This is most likely due to the greater degree of phase separation present in ET1. ET1 is less likely to exhibit hydrogen bonding between the urethane hard segment and the ether oxygen in the soft segment compared to the hydrogen bonding potential between the urethane hydrogen and the polyester carbonyl of ES2. Less order within the hard segment and greater phase mixing may be present in ES2, resulting in a lower temperature associated with the polymer melt. ET1 exhibits better low-temperature flexibility and greater heat stability due to the enhanced phase separation of the polymer.

Fig. 4 shows the DSC scans of ES2 prior to, and following, strain aging at 100% elongation for 240 h. The strain aging was conducted at ambient temperature. The solid line represents the strain-aged specimen. The two endothermic transitions observed in the unaged specimen are replaced by a very broad endothermic transition after strain aging, which spans the entire temperature range of the original transitions. The very prominent lower temperature endothermic transition disappears after the sample is subjected to

Table 2
Endothermic transitions of unaged model polyurethane elastomers [a]

Sample	T_g (°C)	Endo 1 peak, T/°C	Endo 1 ΔH, (J/g)	Endo 2 peak, T/°C	Endo 2 ΔH, (J/g)
ES1	−34	60.4	1.5	117.1	4.9
ES2	−32	62.8	2.6	137.4	6.9
ES3	−29	66.5	2.3	145.7	10.7
ET1	<−35	72.0	3.0	156.8	4.1

[a] Data was obtained using a TA Instruments 2920 DSC under a nitrogen purge of 50 cc/min, and a heating rate of 10°C/min.

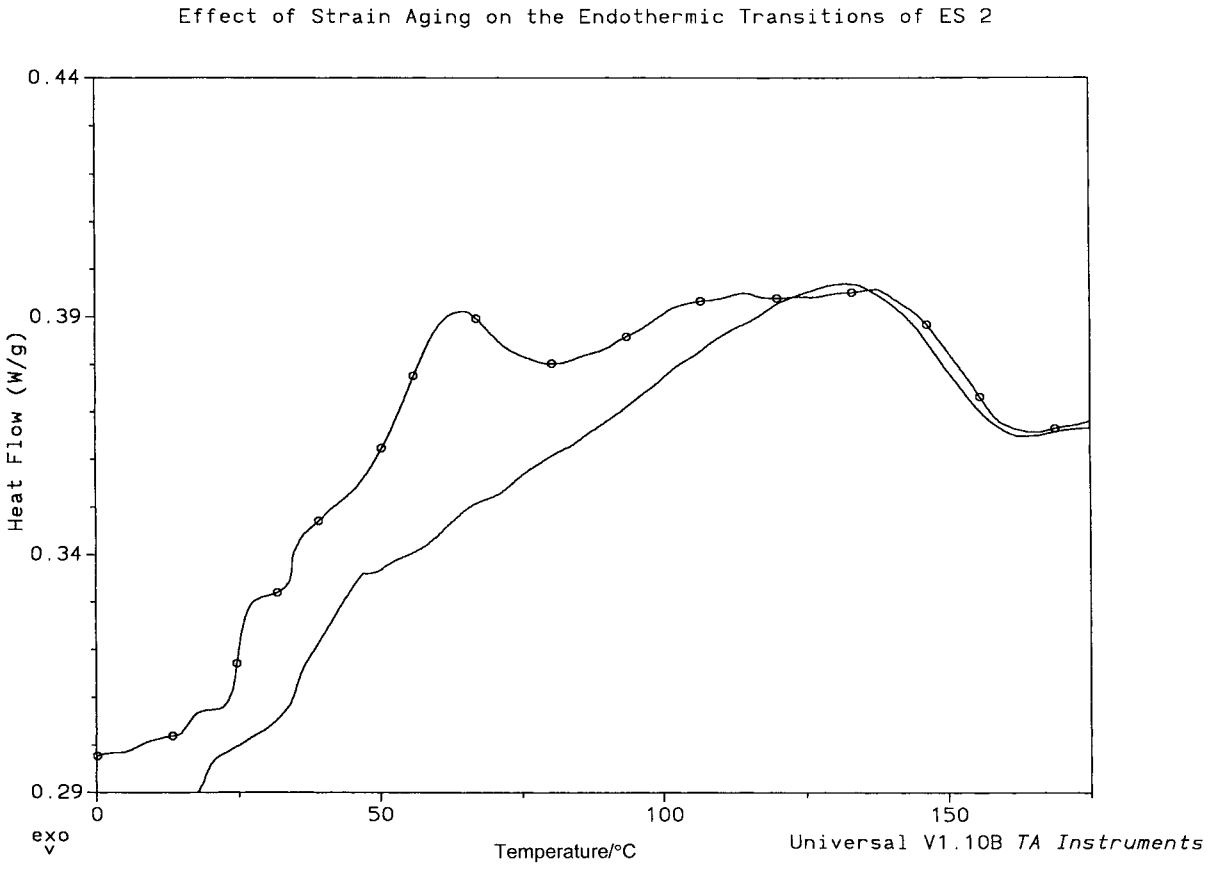

Fig. 4.

strain aging. This data suggests that when the materials are strained (followed by 1 h of relaxation at room temperature) the two phases originally present in the polymer are diminished and some change in morphology has taken place. This observation was made for all of the model polymers that were studied.

When the polymers are annealed for 240 h at 76°C without induced strain, a very different result is observed. Fig. 5 shows the DSC scan of ET1 before, and after, heat aging at 76°C. As shown by the solid line, annealing causes an increase in the onset and peak temperatures of the lower temperature transition and results in a sharper transition. This suggests improved phase separation between the hard and soft segments or improved short-range order of the hard segments. The onset temperature of the higher temperature endotherm is increased significantly as well; however, the peak temperature is unaffected. The endothermic transitions have narrowed considerably, indicating improved order or phase separation.

Dynamic mechanical properties were studied to determine the relationship between tan δ, loss modulus (E'') and storage modulus (E') and the morphology of strain aged and unaged model polymers. Fig. 6 shows the tan δ peak magnitude and the corresponding T_g of the model polyester TPEs. The data show that the tan δ peak magnitude and T_g are sensitive to the composition of the TPUs. As the hard segment content of the three ester polymers is increased, their tan δ peak magnitude decreases and the glass-transition temperature increases. This trend is consistent with polymers that have increasing amounts of crystallinity [18]. The increasing hard segment content results in larger hard microcrystalline domains that restrict the molecular motion of the soft segment thereby increasing the glass-transition temperature. The height of the

Fig. 5.

tan δ peak is related to the amount of the amorphous material present [18]. Since ET1 has the same molar percentage of soft segment content as ES2, the tan δ peak magnitude of these two polymers is essentially the same as shown in Fig. 7. However, the T_g of these polymers is profoundly different, a fact that can be attributed to the greater degree of rotational freedom associated with the ether linkage.

An interpretation of the tan δ peak magnitude after the polymers have undergone strain aging is difficult because the storage modulus, E', also changes as a result of strain. This reflects the complexity of the morphological changes that occur in these materials as a result of induced strain elongation. The transition temperature associated with the tan δ peak is shown in Table 3 for the polyester TPUs. The temperature of the tan δ transition increases for all of the polyester polyurethanes after strain aging up to 200% elongation. This increase in glass-transition temperature suggests that some degree of phase mixing has occurred. This increase in T_g is not observed after

Table 3
Glass-transition temperature [a] of model polyester polyurethane elastomers strain aged 240 h at ambient temperature

Percent strain	ES1 T_g/°C	ES2 [b] T_g/°C	ES3 T_g/°C
0%	−12.2	−2.5	−0.5
100%	−8.7	0.03	6.4
200%	−5.7	0.9	9.5

[a] T_g is defined as the temperature corresponding to the tan δ peak. Imass, Inc. autovibron data were taken at 110 Hz. A heating rate of 2°C/min was used.
[b] The change in T_g observed for ES2 was smaller than that observed for ES1 and ES3. This observation is probably the result of poor temperature control of the instrument near 0°C, due to the change from a cooling program to a heating program in the instrument software.

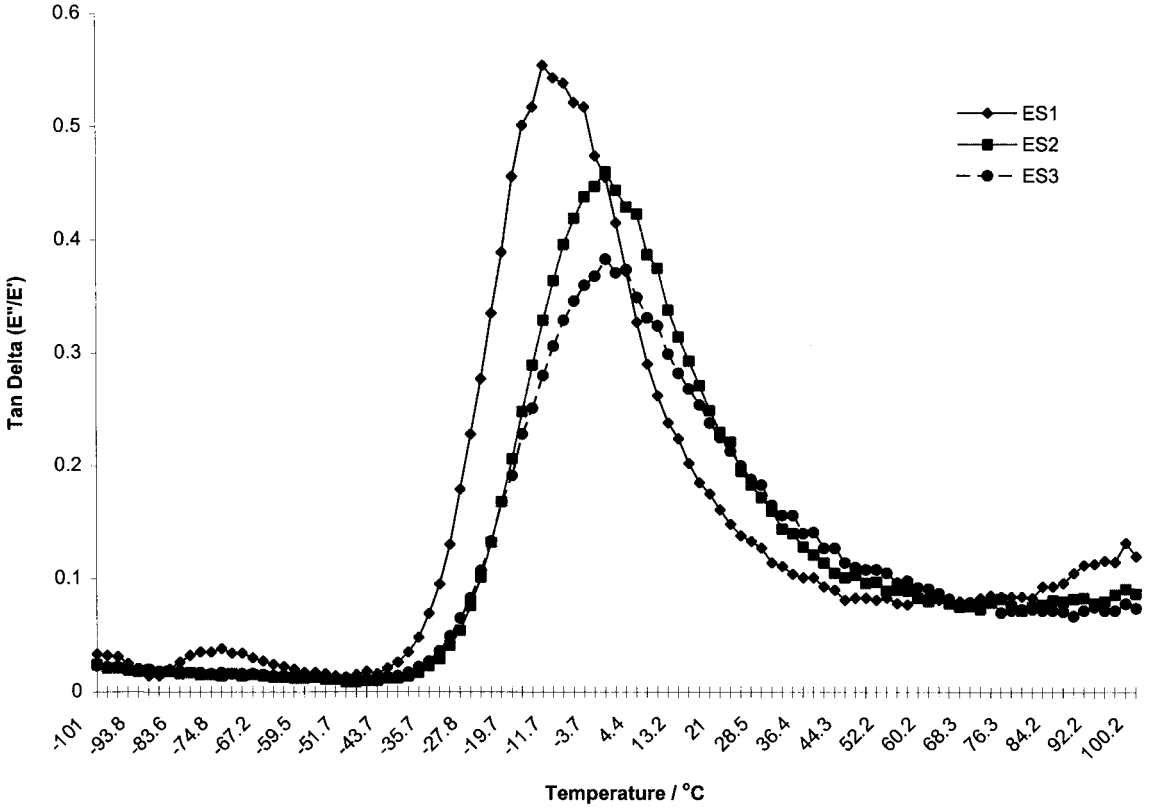

Fig. 6.

200% elongation. In all three of the polyester TPEs, the tan δ magnitude increases after 100% strain elongation. Beyond 100% elongation these values vary, without showing a consistent trend.

Table 4 shows the tan δ peak magnitude and corresponding transition temperature for ET1. Unlike ES2, the polyether polyurethane exhibits a decreasing trend in tan δ peak magnitude with increasing levels of strain aging. Although the temperature associated with the tan δ transition initially increases, beyond 100% elongation the transition temperature begins to decrease without showing a clear trend. Though the tan δ peak magnitude shows a decreasing trend for ET1 with increasing levels of strain aging, the loss modulus of this same material shows the opposite trend. The magnitude of E'' increases and broadens as a result of increasing strain levels, as shown in Fig. 8. The polyester polyurethanes do not exhibit notable changes in tan δ or E'' peak magnitude as a result of strain aging; however, they do show increases in T_g after 100% and 200% elongations.

Table 4
Tan δ peak magnitude and T_g of ET1 strain aged 240 h at ambient temperature [a]

Percent strain	Tan δ peak magnitude	T_g/°C
0%	0.454	−21.6
100%	0.431	−16.9
200%	0.429	−18.6
300%	0.417	−21.7
400%	0.408	−19.6

[a] Imass, Inc. autovibron data were taken at 100 Hz. A heating rate of 2°C/min was used.

DMA distinguishes the response of the polyester and polyether TPUs with respect to strain aging. The differences seen in the DMA data for ES2 and ET1 may be the result of greater interaction between the hard and soft domains of ES2, arising from greater

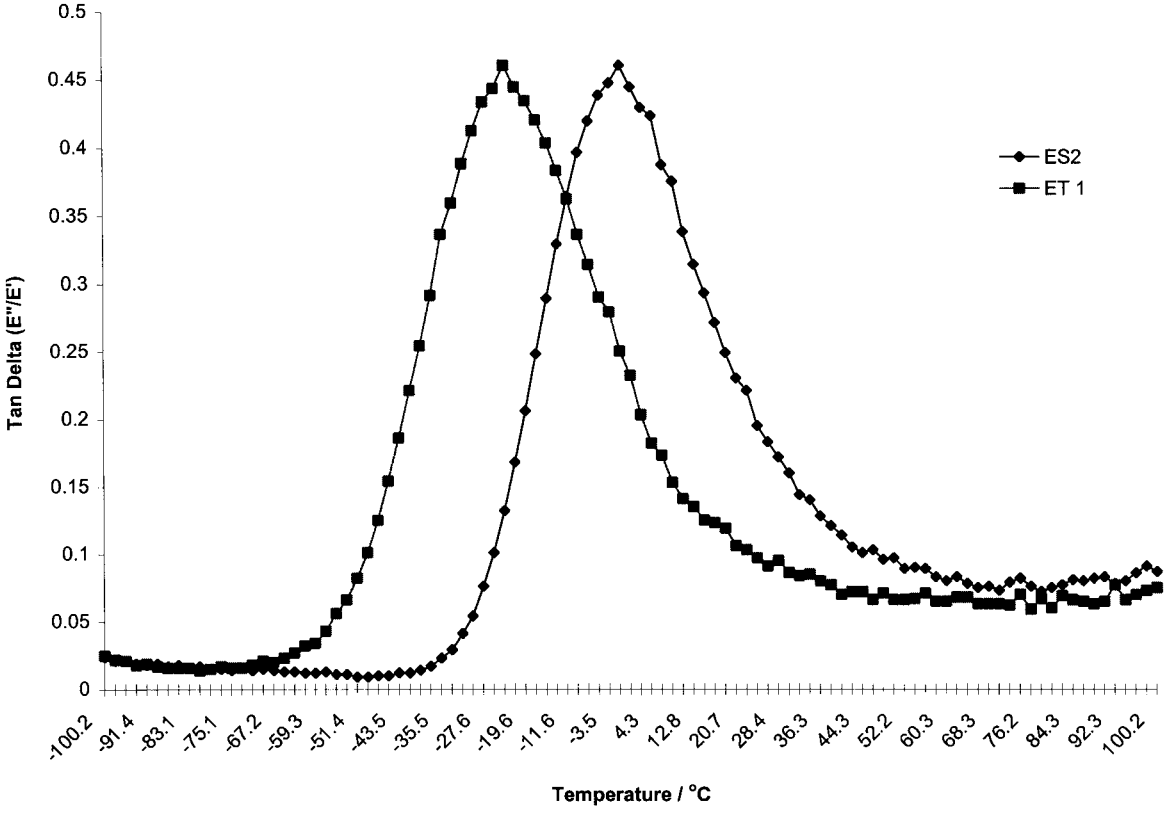

Fig. 7.

potential of hydrogen bonding between the ester carbonyl and the urethane hard segments. The greater potential for hydrogen bonding between hard and soft domains in ES2 may further complicate the interpretation of the morphological changes that are brought about by the strain aging. The consistent trend observed in the dynamic properties of ET1 may be due to a lesser degree of interaction between the hard and soft domains of the polyether based polymer. Greater separation of hard and soft domains in ET1 is supported by the DSC data which shows that ET1 has a higher temperature associated with the hard domain disordering/melt. Since the percentage of hard segment is the same in both ES2 and ET1, the higher dissociation temperature of ET1 is most likely a result of more ordered hard segment domains. This is a good indication that there is less 'free' hard segment available to interact with the soft segment domains in ET1. This may explain why ET1 exhibits a clear trend in dynamic properties compared to ES2.

ET1 exhibits broadening of the peak E'' transition and a slight lowering of the E'' peak temperature after strain aging for 240 h at ambient temperature. Peak broadening is generally associated with phase mixing in segmented polymers [19]. ET1 also shows an increase in E'' peak magnitude at higher levels of strain elongation. If strain aging was causing crystallization, the temperature of peak E'' would increase and the magnitude of E'' would decrease [20]. Therefore, the DMA data confirms that soft segment strain crystallization does not occur in ET1. The increase in the magnitude of E'' of ET1 may be the result of increased hysteresis of the polymer due to the reordering of the phases or plastic deformation that has occurred within the hard domains as a result of the strain elongation.

Tensile and abrasion tests were performed on the model polymers. Tensile strength and modulus at 100% elongation were performed using an Instron machine according to ASTM D 412. Both the

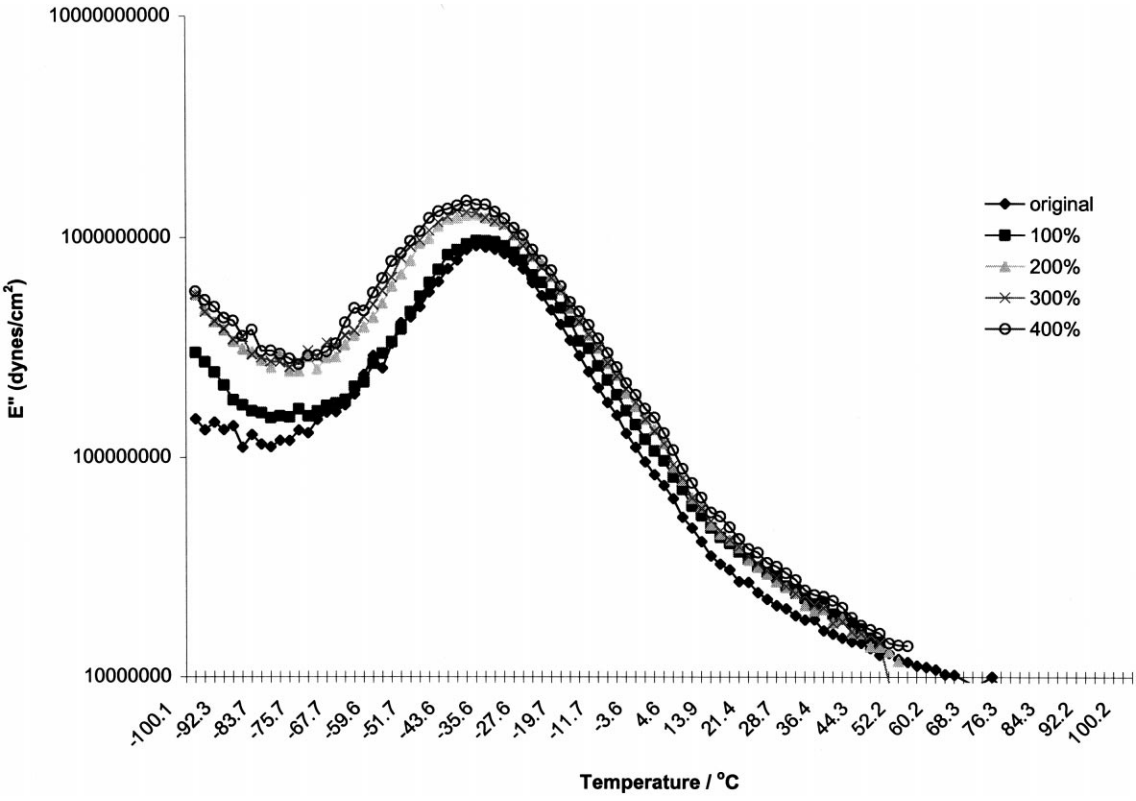

Fig. 8.

properties increased with increasing hard segment content of the unaged TPEs while the ultimate elongation decreased. After the samples were strain aged at ambient temperature and allowed to relax for 1 h, the residual elongation was measured. ES3 exhibited residual elongation ranging between 50% and 135%. Tensile strength and modulus at 100% elongation increased with increasing levels of strain aging and the elongation at break (ultimate elongation) decreased sharply. Residual elongation, modulus at 100% elongation and the ultimate elongation of ES3 are shown in Table 5. The results are consistent with a greater degree of hard segment dispersed within the soft segment domains as strain aging levels increase, correlating with the results obtained using DSC and DMA.

Abrasion resistance is represented by the abrasion rating index (ARI) which is described in the ISO Method 4649. The ARI is a dimensionless value calculated from the mass loss of the sample as a result of abrasion. ARI is directly proportional to abrasion resistance. Abrasion resistance of unstrained polyurethane elastomers improves with increasing hard segment content. However, the abrasion resistance of the model polymers decreases after the materials are strain aged. Fig. 9 shows ARI with respect to levels of strain aging for ES2 and ET1. Fig. 9 shows that ET1 exhibits superior abrasion resistance to ES2 after all aging conditions. These results may be explained by

Table 5
Modulus at 100% elongation and ultimate elongation of ES3 strain aged 240 h at ambient temperature

Strain aging, %	Residual elongation, %	Modulus at 100% elongation / (MPa)	Ultimate elongation, %
0	—	8.7	533
100	50	14.8	343
200	113	27.7	220
300	135	22.3	226

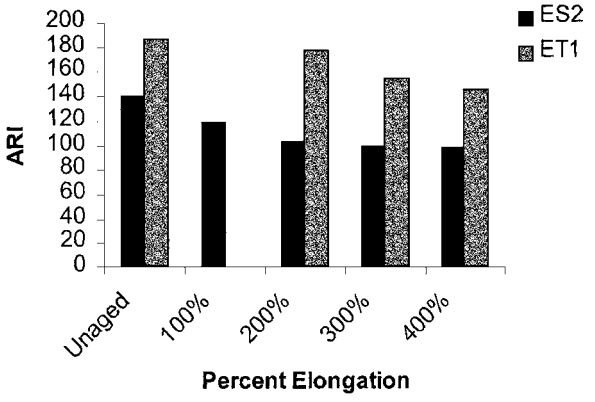

Fig. 9.

the DSC data indicating the greater phase separation of ET1 and by the dynamic data which shows a more uniform trend in loss properties of ET1 after strain aging. Clearly, the thermal techniques and mechanical tests used to characterize these materials suggest that these materials respond differently to induced strain. Future experiments are planned utilizing small-angle neutron scattering (SANS) to investigate the different mechanisms of domain re-ordering that take place in these materials as a result of strain aging.

5. Conclusions

Numerous model TPEs were characterized before, and after, varying degrees of strain aging to study the effect of strain on the polymer morphology and mechanical properties. DSC, DMA, tensile properties and abrasion properties were evaluated. The data clearly shows that strain aging disrupts the domain structure significantly enough to cause a reduction in abrasion resistance. This disruption in the domain structure may involve phase mixing with, or without, hydrogen bonding taking place between the hard and soft domains, a breaking up of the hard domain microstructure and dispersion of hard segments within the soft domain, or plastic deformation of the hard domains. It is possible that the polyester- and polyether-based polyurethanes may exhibit different domain re-ordering mechanisms. Strain aging results in a merging of the endothermic transitions observed in the DSC scans.

The DMA data indicated that the interaction between the hard and soft domains as a result of strain aging is quite complex. This is especially true with the polyester TPE which does not show a consistent trend in tan δ or E'' with increasing strain. This may be due to the lower degree of phase separation present in the polyester TPE compared to the polyether TPE based on the same percentage of hard segment, and the greater potential of hard segment/soft segment interaction of the polyester based TPE due to potential hydrogen bonding between the urethane hard segment and the soft segment carbonyl. Data relating to tan δ show an increase in T_g up to 200% strain elongation for ES2. Heat aging the TPEs without strain elongation is shown to enhance domain ordering/phase separation and results in improved abrasion resistance. A higher degree of domain ordering within the polymer and higher extensibility before failure appear to be most related to improved abrasion properties. Future studies are planned using small-angle scattering to better understand the different domain structure re-ordering of polyester- and polyether-based TPEs with respect to induced strain aging.

Acknowledgements

The authors would like to acknowledge Dr. Larry Hewitt of B.F. Goodrich for providing the model polymers used in this research and for his many helpful discussions on aspects of polymer chemistry and polymer characterization.

References

[1] G.M. Estes, R.W. Seymour, S.L. Cooper, ACS Sym. Proc. 11 (1970) 516.
[2] R.W. Seymour, S.L. Cooper, J. Polym. Sci. 46 (1974) 69.
[3] H.S. Lee, S.L. Hsu, J. Polym. Sci. Part B: Polym. Phys. 32 (1994) 2085.
[4] N. Reynolds, H.W. Spiess, H. Hayden, H. Nefzger, C.D. Eisenbach, Macromol. Chem. Phys. 195 (1994) 2855.
[5] C.R. Desper, N.S. Schneider, J.P. Jasinski, Macromolecules 18 (1985) 2755.
[6] M. Shibayama, Y. Ohki, T. Kotani, S. Nomura, Polym. J. 19 (1987) 1067.
[7] J.I. Mardel, A.J. Hill, K.R. Chynoweth, M.E. Smith, C.H.J. Johnson, T.J. Bastow, Wear 162–164 (1993) 645.
[8] R. Seymour, S. Cooper, Macromolecules 6 (1973) 48.

[9] C. Hepburn, Polyurethane Elastomers, Applied Science, New York, 1982, pp. 1–49.
[10] A. Awater, in G. Ortel (Ed.), Polyurethane Handbook, Hanser, New York, 1985, pp. 372–376.
[11] K.W. Chau, P.H. Geil, Polym. 26 (1985) 490.
[12] H. Wenchun, J. Koberstein, J. Polym. Sci. Polym. Phys. 32 (1994) 47.
[13] J. Koberstein, J.A. Galambos, L. Leung, Macromolecules 25 (1992) 6195.
[14] R. Seymour, S. Cooper, J. Polym. Sci. 46 (1974) 69.
[15] Y. Li, T. Gao, J. Liu, K. Linliu, C.R. Desper, Macromolecules 25 (1992) 7365.
[16] R. Seymour, S. Cooper, Polym. Lett. 9 (1971) 689.
[17] L.M. Leung, J.T. Koberstein, Macromolecules 19 (1986) 706.
[18] T. Murayama, Dynamic Analysis of Polymeric Material, Elsevier Scientific, New York, 1978, pp. 61–68.
[19] W.-Y. Chiang, D.-M. Chang, Polym. Internat. 39 (1996) 55.
[20] T. Murayama, Dynamic Analysis of Polymeric Material, Elsevier Scientific, New York, 1978, p. 79.